

## Three body decays of $D^0$ and $D_S$ mesons

Antimo Palano  
INFN and University of Bari, Italy  
(for the *BABAR* Collaboration)

### Abstract

Results are presented on the study of three body decays of  $D^0 \rightarrow K_S^0 h^+ h^-$ , where  $h = \pi/K$  and  $D_S^\pm \rightarrow K_S^0 K_S^0 \pi^\pm$ . The data have been collected by the BaBar experiment at SLAC and are extracted from continuum  $e^+e^-$  annihilations at the  $\Upsilon(4S)$  energy.

Presented at Hadron 2001, IX International Conference on Hadron Spectroscopy  
August 25–September 1, 2001, Protvino, Russia

---

*Stanford Linear Accelerator Center, Stanford University, Stanford, CA 94309*

Work supported in part by Department of Energy contract DE-AC03-76SF00515.

# 1 Introduction

New generation experiments are providing large data sets for charm physics with statistics which supersede most previous measurements. The Dalitz plot analyses of 3-body charm decays have been performed in the past but these new large and clean samples will allow high precision measurements that were never before possible.

The Dalitz plot analysis of three-body decays is a relatively new technique in development for charm physics studies. This method of analysis is the most complete way of analyzing the data since it allows measurement of both decay amplitudes and phases. The final state is the result of the interference of all intermediate states. The significant results provided by these studies are:

- Accurate measurements of branching fractions.
- A study of Final State Interactions.
- A study of CP violation in rates and decay amplitudes.
- New input to several old unsolved problems in light meson spectroscopy, in particular to the scalar mesons puzzle.

Factorization models assume the weak decay amplitudes to be real. The fact that the observed amplitudes have a relative complex phase is a consequence of final state interaction.

CP violation is expected to be small in charm decays ( $\approx 10^{-3}$ ) [1]. Two amplitudes with different phases are needed:

$$Ae^{i\delta_A} + Be^{i\delta_B}$$

In singly Cabibbo-suppressed decays penguin terms may provide a weak phase, while Final State Interactions provide a strong phase shift. Under CP the weak phases change sign but the strong ones do not. Any difference between  $D$  and  $\bar{D}$  in the Dalitz plot would be evidence for CP violation.

Throughout this paper charge conjugate modes, where not explicit, are implied.

## 2 The BaBar Experiment

The PEP-II Collider is an asymmetric storage ring which collides 9 GeV electrons with 3.1 GeV positrons with a peak luminosity of  $4.2 \times 10^{33} \text{ cm}^{-2} \text{ s}^{-1}$ . The  $\Upsilon(4S)$  resonance is produced with  $\beta\gamma = 0.56$  in the laboratory frame at zero crossing angle. Details on the layout of the apparatus, trigger conditions and data processing can be found in previous publications [2].

The  $\Upsilon(4S)$  resonance sits on a large continuum background with a contribution from  $e^+e^- \rightarrow c\bar{c}$  of 1.30 nb. The power of BaBar for studying charm physics is based on:

- Relatively small combinatorics because of  $e^+e^-$  interactions.
- Good vertexing.
- Good Particle Identification.
- Detection of all possible final states, with charged tracks and  $\gamma$ 's.
- Very high statistics.

The BaBar experiment is continuously collecting data. This work is based on the data taken during 1999/2000 and corresponds to an integrated luminosity of  $\approx 23 \text{ fb}^{-1}$  unless otherwise specified.

### 3 Study of $D_S^+ \rightarrow K_S^0 K_S^0 \pi^+$

The resonance  $f_J(1710)$  has been measured with spin 0 or 2 in different experiments. It has been a candidate for being the lowest lying scalar or tensor glueball. It has been observed in  $J/\psi$  decay, central production and  $\gamma\gamma$  collisions [3]. Details on the selection criteria used to isolate the  $K_S^0 K_S^0 \pi^+$  final state can be found in ref. [4]. The  $K_S^0 K_S^0 \pi^+$  mass spectrum (relative to an integrated luminosity of  $18.4 \text{ fb}^{-1}$ ) is plotted in fig. 1 and shows signals from  $D^+$  and  $D_S^+$ . The background

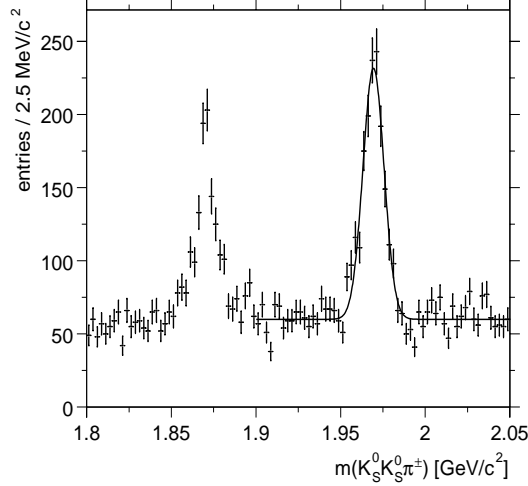


Figure 1:  $K_S^0 K_S^0 \pi^+$  mass spectrum.

subtracted Dalitz plot and its  $K_S^0 K_S^0$  projection are shown in fig. 2. Strong accumulations in the region of the  $K^*(892)$  can be seen. A preliminary Dalitz plot analysis shows that the data cannot be described with  $K^*(892)$  alone but require the presence of the  $D_S^+ \rightarrow f_J(1710)\pi^+$  final state.

### 4 Selection of $D^0 \rightarrow K_S^0 h^+ h^-$

$D^0$ 's are required to come from a  $D^{*+}$  decay:

$$\begin{aligned} D^{*+} &\rightarrow D^0 \pi^+ \\ &\rightarrow \bar{K}^0 \pi^+ \pi^- \\ \\ D^{*-} &\rightarrow \bar{D}^0 \pi^- \\ &\rightarrow K^0 \pi^+ \pi^- \end{aligned}$$

Therefore the charge of the slow  $\pi$  gives the flavour of the  $D^0$  and that of the  $K^0$  (apart from the contribution from DCSD, which is expected to be  $\approx 10^{-4}$ ).

The selection of the channel starts with the reconstruction of the  $K_S^0$  and  $D^0$  vertices. The slow  $\pi$  are refitted using the beam spot constraint to improve the resolution, (beam spot size:  $\sigma_x = 0.15 \text{ mm}, \sigma_y = 0.05 \text{ mm}, \sigma_z = 8 \text{ mm}$ ). The center of mass momentum of the  $D^0$  ( $p^*$ ) has been required to be greater than  $2.2 \text{ GeV}/c$ .

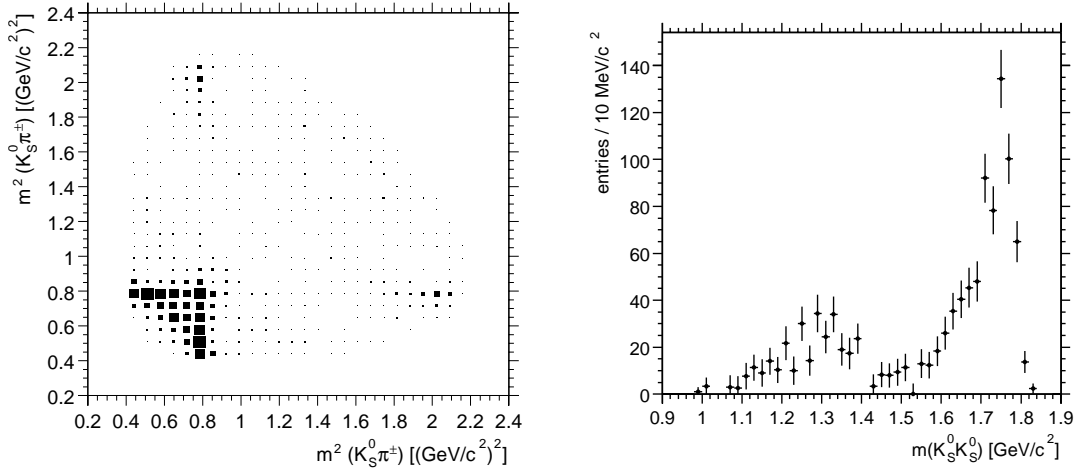


Figure 2: Background subtracted Dalitz plot and  $K_S^0 K_S^0$  projection for  $D_S^+ \rightarrow K_S^0 K_S^0 \pi^+$ .

The mass difference:

$$\Delta m = m(K^0 \pi^+ \pi^- \pi_s) - m(K^0 \pi^+ \pi^-)$$

where the slow pion  $\pi_s$  has a momentum below  $0.6 \text{ GeV}/c$  is plotted in fig. 3. Fig. 3a) and fig. 3b) show respectively the  $\Delta m$  distribution before and after having required a  $2.5 \sigma$  cut around the  $D^0$  mass. Fitting the  $\Delta m$  width using a single Gaussian and a threshold function  $(m - m_{th})^\alpha e^{-\beta m - \gamma m^2}$ ,

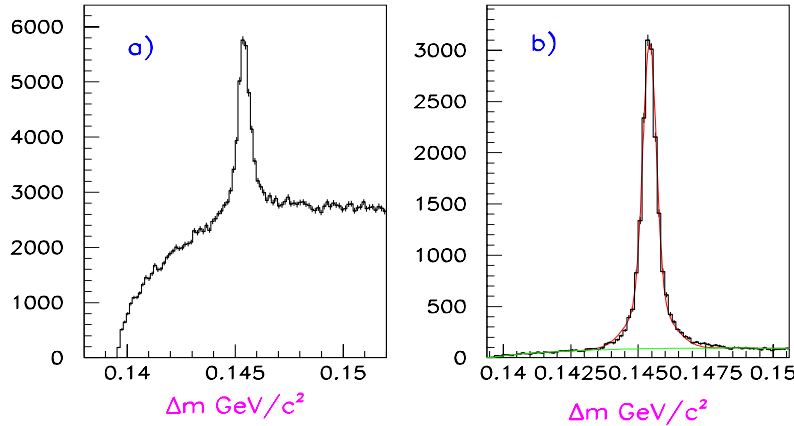


Figure 3:  $\Delta m$  distributions for  $K_S^0 \pi^+ \pi^-$  a) before and b) after a  $D^0$  mass cut at  $2.5\sigma$ .

we obtain  $\sigma = 326 \pm 10 \text{ keV}/c^2$ . Performing now a  $2.0 \sigma$  cut on  $\Delta m$  we obtain the  $m(K_S^0 \pi^+ \pi^-)$  shown in fig. 4. The  $D^0$  width obtained fitting only one Gaussian and a linear background is:  $\sigma = 6.3 \pm 0.1 \text{ MeV}/c^2$ .

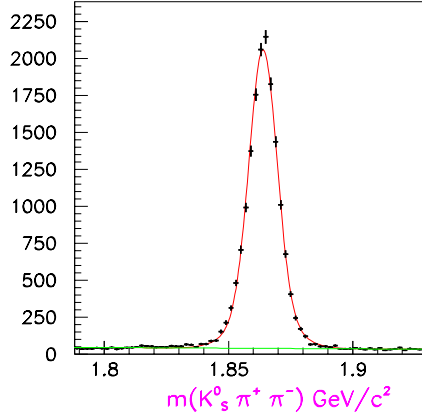


Figure 4:  $K_S^0\pi^+\pi^-$  mass distribution after a  $D^{*+}$  cut at  $2\sigma$ .

The Dalitz plot of  $D^0 \rightarrow K_S^0\pi^+\pi^-$ , obtained by selecting events within  $2.5\sigma$  of the  $D^0$  mass, is shown in fig. 5 (15753 events) and its projections are shown in fig. 6. The background fraction, estimated to be 4.1 %, has not been subtracted. This Dalitz plot reveals a complex structure. Several intermediate resonant states involving  $K^{*+}(892)$ ,  $K_0^{*+}(1430)$ ,  $\rho^0(770)$ ,  $f_0(980)$ ,  $f_0(1370)$  resonances can be seen. Strong interferences can also be seen. In particular,  $f_0(980)$  resonance shows up as a uniform horizontal depletion suggesting interference with a broad scalar resonance.

## 5 Selection of $D^0 \rightarrow K_S^0 K^\pm \pi^\mp$

The decay  $D^0 \rightarrow K_S^0 K \pi$  contains two possible  $D^0$  decay modes:

$$D^0 \rightarrow K^0 K^- \pi^+ \quad (a)$$

$$D^0 \rightarrow \bar{K}^0 K^+ \pi^- \quad (b)$$

The charge of the pion separates the two decay modes. Diagrams contributing to the two decay channels are shown in fig. 7.

The channels have been isolated using similar cuts on the corresponding  $\Delta m$  distribution. Requiring one of the two charged tracks to be positively identified as a kaon we obtain the  $K_S^0 K \pi$  mass distributions for the two decay modes shown in fig. 8.

The fitted widths and yields obtained using only one Gaussian and a linear background are the following:

$$(a) \quad D^0 \rightarrow K^0 K^- \pi^+ : \quad (6.0 \pm 0.1) \text{ MeV}/c^2 \quad 2335 \text{ events}$$

$$(b) \quad D^0 \rightarrow \bar{K}^0 K^+ \pi^- : \quad (5.1 \pm 0.1) \text{ MeV}/c^2 \quad 731 \text{ events}$$

The above yields indicate that branching fractions for the above  $D^0$  decay channels are different.

The two Dalitz plots are shown in fig. 9 and their projections are shown in fig. 10. The background fractions for decays a) and b) have been estimated to be 4 % and 5% respectively and have not been subtracted.

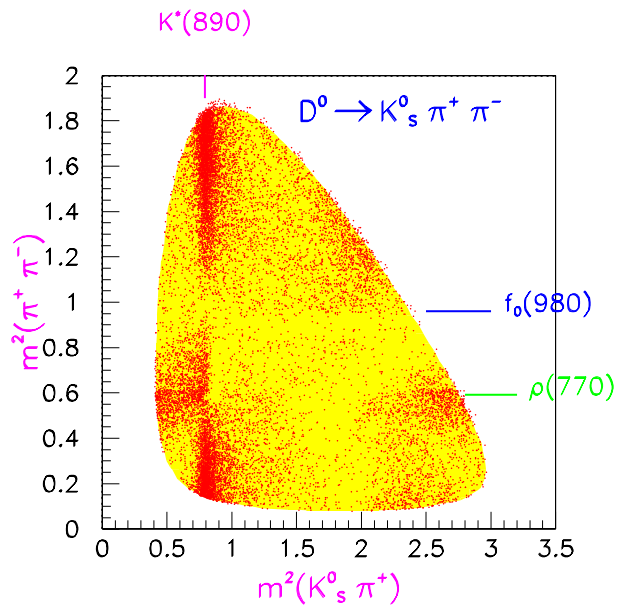


Figure 5:  $K_S^0 \pi^+ \pi^-$  Dalitz plot with no background subtraction.

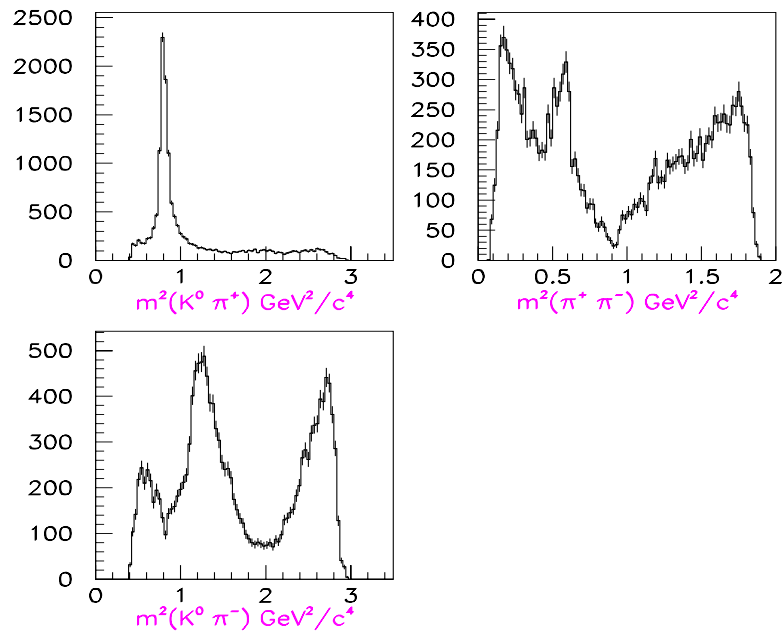


Figure 6:  $K_S^0 \pi^+ \pi^-$  Dalitz plot projections.

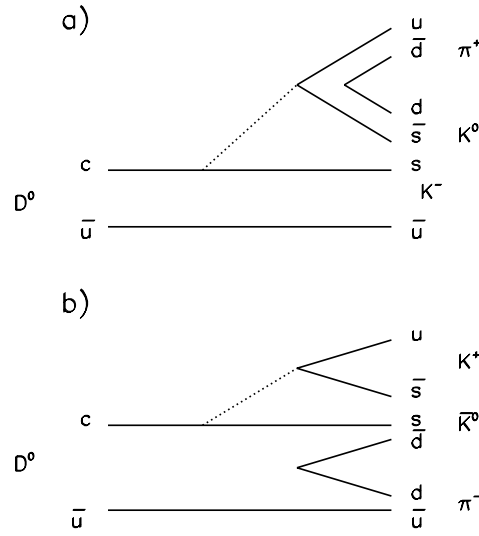


Figure 7: Diagrams which contribute to the two different  $D^0$  decay modes to  $K_S^0 K \pi$ .

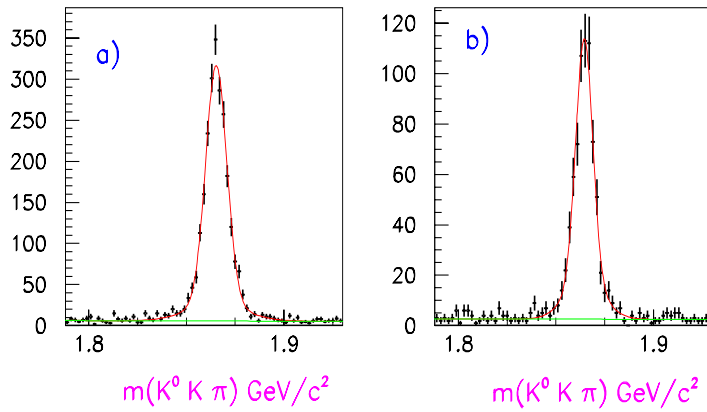


Figure 8: a)  $D^0 \rightarrow K^0 K^- \pi^+$  and b)  $D^0 \rightarrow \bar{K}^0 K^+ \pi^-$  signals.

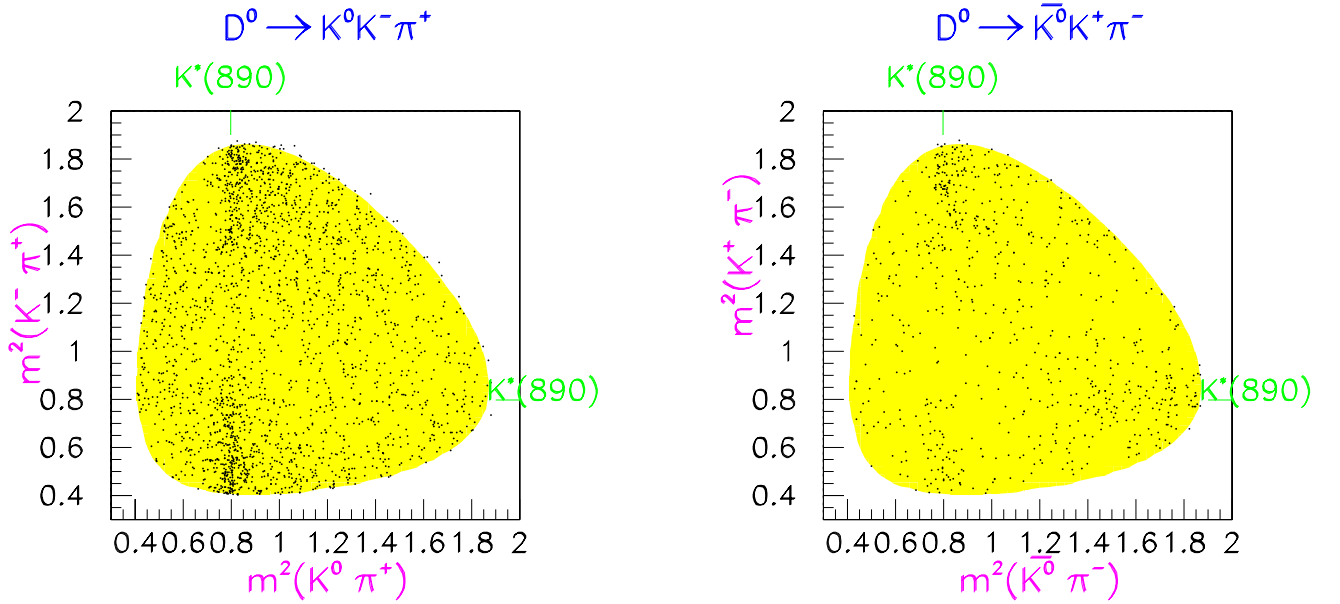


Figure 9: a)  $D^0 \rightarrow K^0 K^- \pi^+$  and b)  $D^0 \rightarrow \bar{K}^0 K^+ \pi^-$  Dalitz plots with no background subtraction.

The decay  $D^0 \rightarrow K^0 K^- \pi^+$  is dominated by  $K^{*0} K^-$  with a small contribution from  $\bar{K}^{*0} K^0$ . We also observe the presence of broad structure. The decay  $D^0 \rightarrow \bar{K}^0 K^+ \pi^-$  shows more symmetric  $K^{*-} K^+$  and  $K^{*0} \bar{K}^0$  contributions.

## 6 Selection of $D^0 \rightarrow K_S^0 K^+ K^-$

The channel has been isolated performing a similar  $\Delta m$  cut and requiring at least one of the two charged tracks to be positively identified as a kaon. The  $K_S^0 K^+ K^-$  mass spectrum is shown in fig. 11.

The  $D^0$  width obtained fitting the mass spectrum with one Gaussian and a linear background is  $(3.7 \pm 0.1) \text{ MeV}/c^2$  and the yield is 2089 events.

The Dalitz plot of  $D^0 \rightarrow K_S^0 K^+ K^-$  is shown in fig. 12 and contains a background fraction of 3% (not subtracted). The corresponding projections are shown in fig. 13.

The presence of intermediate states involving  $\phi$ ,  $f_0(980)$  and  $a_0(980)$  resonances is clearly visible.

## 7 Conclusions

Charm Physics can be performed at B-factories with high statistics and small backgrounds. The Dalitz plot analysis as well as measurements of CP asymmetries in the decay amplitudes and rates for different charmed mesons are in progress.

In the near future, Charm Physics will be dominated by B-factories and  $\tau$ /charm factories. Present available statistics for Dalitz charm decays from fixed target and B-factories are:  $1-5 \times 10^4$

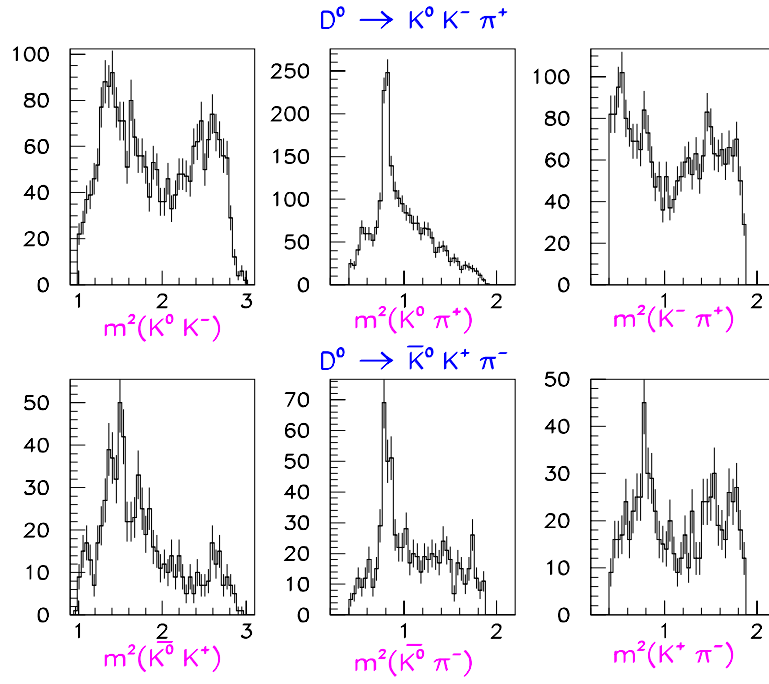


Figure 10: First row:  $D^0 \rightarrow K^0 K^- \pi^+$  Dalitz plot projections. Second row:  $D^0 \rightarrow \bar{K}^0 K^+ \pi^-$  Dalitz plot projections.

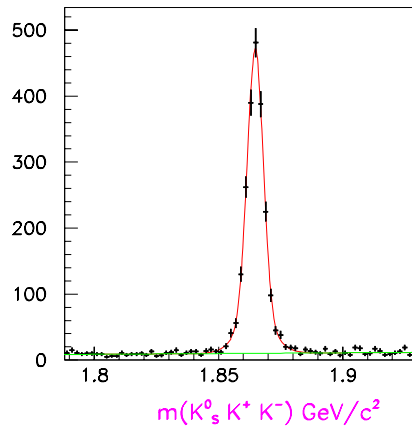


Figure 11:  $K_S^0 K^+ K^-$  mass spectrum

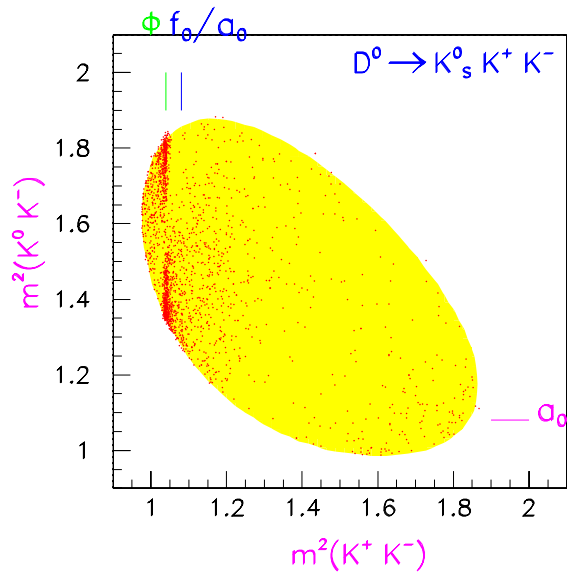


Figure 12:  $D^0 \rightarrow \bar{K}^0 K^+ K^-$  Dalitz plot.

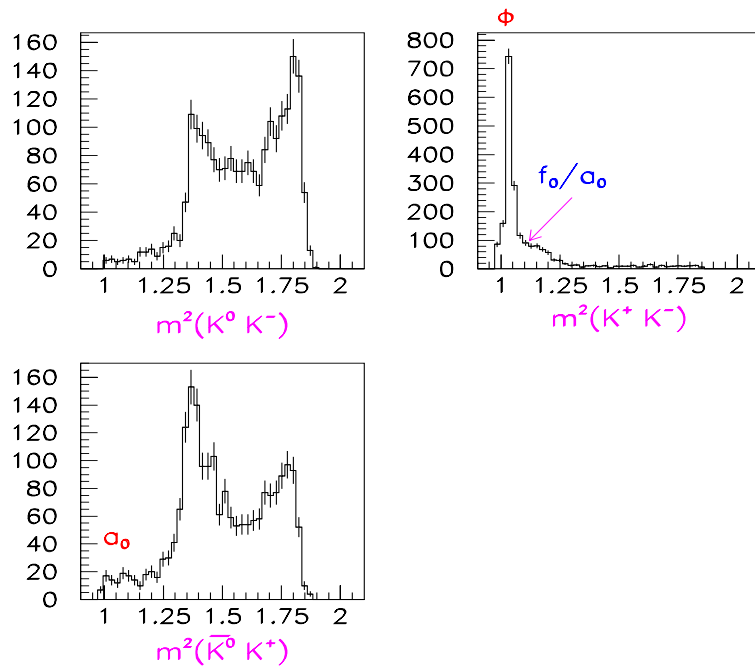


Figure 13:  $D^0 \rightarrow \bar{K}^0 K^+ K^-$  Dalitz plot projections.

events for Cabibbo allowed,  $1\text{--}10\times 10^3$  events for Cabibbo suppressed and 50–300 events for double Cabibbo suppressed decays.

Given the large data samples being accumulated, we expect in the next few years an increase of these yields by a factor 20. This will allow charm physics to be rewritten with errors on branching fractions reduced by more than a factor 10.

## References

- [1] M. Golden and B. Grinstein, Phys. Lett. **B222** 501 (1989).
- [2] B. Aubert et al., The BaBar Detector, SLAC-PUB-8569, hep-ex/0105044, to appear in NIM.
- [3] D.E. Groom et al., The European Physical Journal C15 (2000) 1.
- [4] T. Deppermann (BaBar Collaboration), Dalitz Analyses of  $D_S^\pm \rightarrow K_S^0 K_S^0 \pi^\pm$  and  $D_S^\pm \rightarrow \pi^+ \pi^- \pi^\pm$ , these proceedings.